Eukaryotic Cell

Novel Bilobe Components in Trypanosoma brucei Identified Using Proximity-Dependent Biotinylation

Brooke Morriswood, Katharina Havlicek, Lars Demmel, Sevil Yavuz, Marco Sealey-Cardona, Keni Vidilaseris, Dorothea Anrather, Julius Kostan, Kristina Djinovic-Carugo, Kyle J. Roux and Graham Warren

Eukaryotic Cell **2013, 12(2):356. DOI: 10.1128/EC.00326-12. Published Ahead of Print 21 December 2012.**

EC
Journals.ASM.org

Novel Bilobe Components in *Trypanosoma brucei* Identified Using Proximity-Dependent Biotinylation

Brooke Morriswood,[a] Katharina Havlicek,[a] Lars Demmel,[a] Sevil Yavuz,[a] Marco Sealey-Cardona,[a] Keni Vidilaseris,[a] Dorothea Anrather,[b] Julius Kostan,[c] Kristina Djinović-Carugo,[c,d] Kyle J. Roux,[e] Graham Warren[a]

Max F. Perutz Laboratories, University of Vienna and Medical University of Vienna, Vienna, Austria[a]; Department for Biochemistry and Cell Biology, Max F. Perutz Laboratories, University of Vienna, Vienna, Austria[b]; Department for Structural and Computational Biology, Max F. Perutz Laboratories, University of Vienna, Vienna, Austria[c]; Department of Biochemistry, Faculty of Chemistry and Chemical Technology, University of Ljubljana, Ljubljana, Slovenia[d]; Children's Health Research Center, Sanford Research/USD, Sioux Falls, South Dakota, USA[e]

The trypanosomes are a family of parasitic protists of which the African trypanosome, *Trypanosoma brucei*, is the best characterized. The complex and highly ordered cytoskeleton of *T. brucei* has been shown to play vital roles in its biology but remains difficult to study, in large part owing to the intractability of its constituent proteins. Existing methods of protein identification, such as bioinformatic analysis, generation of monoclonal antibody panels, proteomics, affinity purification, and yeast two-hybrid screens, all have drawbacks. Such deficiencies—troublesome proteins and technical limitations—are common not only to *T. brucei* but also to many other protists, many of which are even less well studied. Proximity-dependent biotin identification (BioID) is a recently developed technique that allows forward screens for interaction partners and near neighbors in a native environment with no requirement for solubility in nonionic detergent. As such, it is extremely well suited to the exploration of the cytoskeleton. In this project, BioID was adapted for use in *T. brucei*. The trypanosome bilobe, a discrete cytoskeletal structure with few known protein components, represented an excellent test subject. Use of the bilobe protein TbMORN1 as a probe resulted in the identification of seven new bilobe constituents and two new flagellum attachment zone proteins. This constitutes the first usage of BioID on a largely uncharacterized structure, and demonstrates its utility in identifying new components of such a structure. This remarkable success validates BioID as a new tool for the study of unicellular eukaryotes in particular and the eukaryotic cytoskeleton in general.

The trypanosomes are a family of uniflagellated kinetoplastids. All species are parasitic, and a number are human pathogens. The African trypanosome *Trypanosoma brucei* is one such species and is responsible for considerable morbidity and mortality in both people and livestock. It is also the best-studied member of the Trypanosomatida order.

T. brucei exhibits a highly organized cytoskeletal architecture (1). The cell body is a tapered cylinder, maintained by a subpellicular corset of microtubules aligned with their plus ends at the cell's posterior pole (2). In the trypomastigote form, the stage in which *T. brucei* spends the majority of its life cycle, the single flagellum emerges near the posterior end of the cell and is attached lengthwise as far as the anterior cell tip (3). The base of the flagellum is present in a bulb-shaped invagination of the plasma membrane termed the flagellar pocket, which is the site of all exo- and endocytic traffic (4). The basal body that nucleates the flagellar axoneme abuts the flagellar pocket, with the paired probasal body lying orthogonally to it (5). At the top of the flagellar pocket is an electron-dense cytoskeletal barrier element termed the flagellar pocket collar (6). Between the flagellar pocket collar and the site of flagellum exit from the cell body is a vase-shaped region named the flagellar pocket neck (7). The flagellar pocket neck, flagellar pocket, and flagellar membrane are all contiguous with the plasma membrane and represent distinct subdomains of it (3). Originating between the basal body and probasal body is an array of four specialized microtubules that follow a helical path around the flagellar pocket, pass through the flagellar pocket collar and flagellar pocket neck, and parallel the path of the flagellum to the cell's anterior pole (8). A proteinaceous filament runs alongside this microtubule quartet from the flagellar pocket neck region onwards (9). The protein filament and the microtubule quartet together comprise the flagellum attachment zone (FAZ). The FAZ is responsible for adhering the flagellum to the cell body.

Numerous studies have established that the cytoskeleton is essential for normal cell growth of *T. brucei in vitro*. Loss of cytoskeletal proteins cause a variety of morphological, motility, or replicative phenotypes, ranging from aberrant cell shapes and detached flagella to impaired or entirely abrogated cell locomotion and compromised organelle biogenesis and cytokinesis (10–13). Despite this wealth of evidence supporting the role of the cytoskeleton in trypanosome biology, it remains poorly understood due to the intractability of many of its protein components. A good example is the trypanosome bilobe, an enigmatic cytoskeletal structure of unclear function (14). The roughly 2-μm-long bilobe is present in the flagellar pocket neck and partially overlaps with the posterior end of the FAZ (15). There are only two proteins known to exclusively localize to it—TbMORN1 (Tb927.6.4670) and TbLRRP1 (Tb11.01.0680) (15, 16). TbCentrin4 and TbCentrin2 have also been localized to the bilobe but are additionally present on the

Received 21 November 2012 **Accepted** 17 December 2012
Published ahead of print 21 December 2012
Address correspondence to brooke.morriswood@mfpl.ac.at.
M.S.-C. and K.V. contributed equally to the manuscript.
Supplemental material for this article may be found at http://dx.doi.org/10.1128/EC.00326-12.

doi:10.1128/EC.00326-12

basal and probasal bodies at the base of the flagellum (17, 18). Recent light microscopy and electron microscopy work has shown that TbMORN1 and TbLRRP1 colocalize on a fishhook-shaped structure whose hook encircles the flagellar pocket above the flagellar pocket collar and whose stem projects toward the cell anterior. TbCentrin4 is present on a bar that lies alongside the anterior stem of the fishhook-shaped structure, completing a hairpin arrangement (19). It is not clear if the bilobe ensemble of TbMORN1, TbLRRP1, and TbCentrin4 represents two separate structures (fishhook plus bar) or a single entity with discrete subdomains. Despite extensive effort, no new bilobe proteins have been discovered to date (our unpublished data).

The recently developed proximity-dependent biotin identification (BioID) technique shows considerable promise for redressing this methodological shortfall (20). It enables forward biochemical screens for binding partners and near neighbors in a native environment without any requirement for detergent solubility. BioID involves tagging a protein of interest with a modified form of the 35-kDa bacterial biotin ligase BirA, which has been previously adapted for expression in eukaryotic cells (20). The normal reaction mechanism of BirA consists of conjugating nucleotide (in the form of ATP) to biotin in order to generate a highly reactive biotinoyl-5′-AMP intermediate (21). This reactive intermediate is then retained in the active site until the enzyme locates a specific lysine residue in the target sequence on its protein substrate. The sequestered intermediate then reacts with the presented lysine residue, resulting in biotinylation of the target protein. In BioID, a mutant form of the BirA enzyme is used which exhibits an extremely low affinity for the reactive biotinoyl-5′-AMP intermediate (22). Consequently this modified enzyme, designated BirA*, effectively acts as a biotinoyl-5′-AMP synthase and releases molecule after molecule of the intermediate into the surrounding milieu. The principle of BioID is therefore to tag the protein of interest with BirA* and to incubate the cells in excess biotin. The BirA* module proceeds to spit out highly reactive molecules of biotinoyl-5′-AMP, leading to the indiscriminate biotinylation of all proteins in the immediate vicinity of the tagged bait in a proximity-dependent fashion (20). These putative binding partners and near neighbors of the protein of interest can then be affinity purified using streptavidin-coated beads. Owing to the remarkable affinity of the biotin-streptavidin bond (K_d, $\sim 10^{-14}$ M) (K_d, dissociation constant), far harsher lysis conditions can be used than in a conventional affinity purification. As such, cytoskeletal proteins, which normally partition into the detergent-insoluble fraction when weak nonionic detergents such as NP-40 are used, are efficiently solubilized and can be captured. These purified proteins can then be identified by mass spectrometry. A key strength of BioID is therefore the ability to preserve information about interactions while employing very strong detergents for cell lysis. By carrying out Western blots of eluted proteins using horseradish peroxidase (HRP)-conjugated streptavidin, the molecular weights of the most prevalent binding partners and near neighbors can be inferred in advance and compared with the mass spectrometry data (see Fig. S1 in the supplemental material).

The work described here concerns the adaptation of BioID for *T. brucei*. As a discrete and stable cytoskeletal structure with a largely uncharacterized protein composition, the bilobe—via its marker protein TbMORN1—represented an excellent test case for the BioID system. The goal therefore was to identify novel structural components of this cytoskeletal entity. Using BioID, a large number of TbMORN1 candidate binding partners and near neighbors were identified by mass spectrometry. Localization of a selection of the highest-scoring candidates relative to controls resulted in the assignment of seven new bilobe proteins and two new FAZ proteins. Integrating these localizations into our existing ultrastructural knowledge of the bilobe has produced a new model of the structure and supports the notion that it is composed of discrete subdomains.

MATERIALS AND METHODS

Antibodies and reagents. The rabbit polyclonal anti-Myc antibody and mouse monoclonal anti-Myc antibody were purchased from Abcam and Invitrogen, respectively. The anti-TbBILBO1 antibodies have been described previously (19). The anti-TbMORN1 rabbit polyclonal antibodies used in this paper, which were raised against recombinant full-length TbMORN1, are new. In immunoblots of whole-cell lysates from *T. brucei*, the antibodies recognized a single protein of approximately 40 kDa (Fig. 1B). In indirect immunofluorescence assays the antibodies produced a labeling pattern indistinguishable from that observed using the older antibodies (Fig. 1C). These specific signals in immunoblotting and immunofluorescence were both lost when assaying samples from cells depleted of TbMORN1. As such, their performance in immunoblotting and indirect immunofluorescence was identical to or better than that of the older original anti-TbMORN1 antibodies, and no specificity issues are evident (reference 15 and data not shown). Biotin, M280 streptavidin-conjugated Dynabeads, HRP-conjugated streptavidin, AlexaFluor488-conjugated streptavidin, and Dyna-Mag magnet were purchased from Invitrogen. The rabbit anti-LdCentrin4 polyclonal antibody, mouse monoclonal anti-Ty1 (BB2) antibody, and 1B41 anti-FAZ antibody were gifts kindly received from Hira Nakhasi (FDA), Cynthia He (National University of Singapore), and Linda Kohl (Museum National d'Histoire Naturelle).

Generation of the pLEW100_Myc_BirA* plasmid. The Myc_BirA* module was amplified from the pcDNA3.1(−) cloning vector with incorporation of additional restriction enzyme sites by PCR. The module was ligated into the pLEW100 expression vector between the HindIII and BamHI sites to generate the new pLEW100_Myc_BirA* plasmid (Fig. 1A). The complete TbMORN1 open reading frame was subcloned into the vector between the XhoI and AflII sites.

Cell lines, culture, and generation. The procyclic 29-13 strain of *T. brucei brucei* was used for the generation of cells inducibly expressing Myc-BirA*-TbMORN1 (23). The pLEW100_Myc_BirA*-TbMORN1 construct was linearized by digestion with NotI and introduced into 29-13 cells by electroporation. Stable transformants were selected by growth in medium containing 5 μg/ml phleomycin and cloned by limiting dilution. Putative clones were screened as described in Results. The procyclic 427 Lister strain of *T. brucei brucei* was used for candidate protein localization. Cells were cultured in SDM-79 medium supplemented with 7.5 μg/ml hemin and 20% heat-inactivated fetal calf serum (Sigma-Aldrich) at 27°C. 29-13 cells additionally required 15 μg/ml neomycin and 50 μg/ml hygromycin to maintain T7 polymerase and tetracycline repressor transgenes.

Immunofluorescence microscopy. Cells were attached to coverslips by centrifugation (1,800 × *g*, 5 s). Detergent-extracted cells, when required, were prepared by incubating cells in PEME buffer {2 mM EGTA, 1 mM $MgSO_4$, 0.1 mM EDTA, 0.1 M PIPES [piperazine-*N*,*N*′-bis(2-ethanesulfonic acid)]-NaOH, pH 6.9} supplemented with 0.5% NP-40 (vol/vol) for 5 min at room temperature (RT) and then washed with phosphate-buffered saline (PBS). Cells were fixed in 4% paraformaldehyde in PBS (20 min, RT). After fixation, cells were washed with PBS, permeabilized with 0.25% Triton X-100 in PBS (vol/vol) (5 min, RT), washed again with PBS, and blocked in 3% bovine serum albumin (BSA) in PBS (wt/vol) (30 min, RT). Antibody binding steps, coverslip mounting, image acquisition, and image processing have been described previously (19).

Purification of biotinylated proteins. Biotin stock solution (1 mM) in SDM-79 tissue culture medium was made fresh for each experiment. Par-

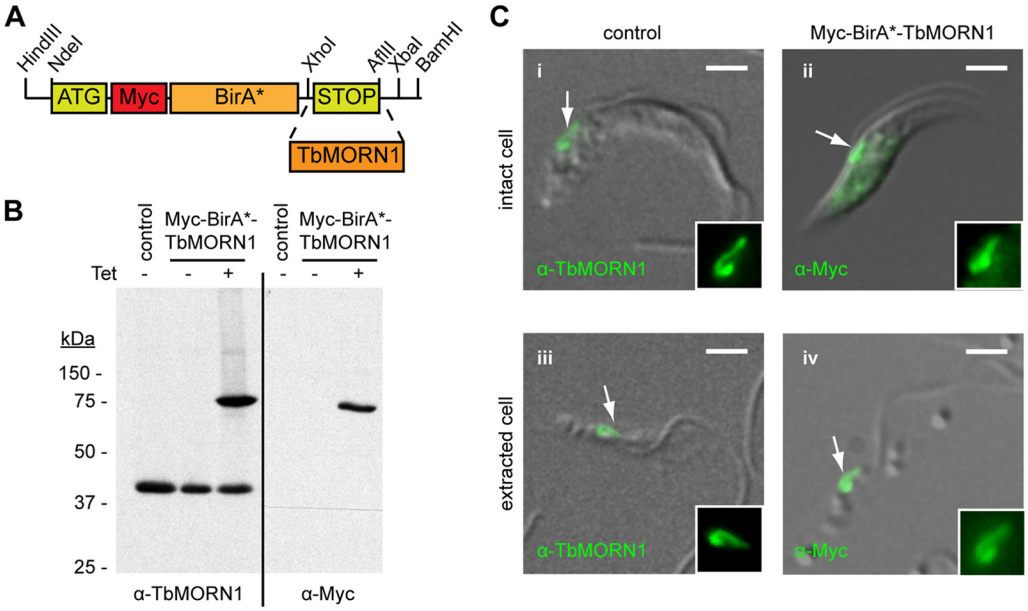

FIG 1 Characterization of Myc-BirA*-TbMORN1-expressing cells. (A) Schematic drawing showing cloning of the *TbMORN1* open reading frame into the modified pLew100_Myc_BirA* plasmid for tetracycline-inducible expression. (B) Myc-BirA*-TbMORN1 is tightly and inducibly expressed. 29-13 cells stably transfected with the pLew100_Myc_BirA*-TbMORN1 plasmid were incubated in the presence or absence of 10 ng/ml tetracycline. Whole-cell lysates were analyzed by immunoblots with either anti-TbMORN1 or anti-Myc antibodies. In untransfected (control) cells and uninduced cells, only the endogenous TbMORN1 (40 kDa) is detected. In the presence of tetracycline, an additional approximately 75 kDa polypeptide was detected by both antibodies. (C) Myc-BirA*-TbMORN1 recapitulates the localization and morphology of the endogenous protein. Untransfected (control) cells or Myc-BirA*-TbMORN1-expressing cells were analyzed by immunofluorescence assay. Intact (panels i and ii) and detergent-extracted (panels iii and iv) cells were labeled with anti-TbMORN1 or anti-Myc antibodies. The bilobe structure is indicated (white arrows, area shown enlarged in insets). Scale bars, 2 μm.

allel cultures of cells (experimental and control) were grown in either the presence or the absence of 10 ng/ml tetracycline overnight to induce Myc-BirA*-TbMORN1 expression. This drug concentration produces mild overexpression of the ectopic copy of the protein. The cultures were then scaled up to final volumes, supplemented with biotin stock solution to a final concentration of 50 μM, and incubated for a further 24 h. The cells were harvested by centrifugation (1,800 × *g*, 5 min, 4°C), washed three times with PBS, and transferred to Eppendorf tubes. The cells were extracted in PEME buffer supplemented with 0.5% NP-40 (vol/vol) (15 min, RT, gentle mixing), and a 5% sample (E1) was taken. Detergent-soluble and -insoluble fractions were then separated by centrifugation (3,400 × *g*, 2 min, RT); a 5% sample was taken of the supernatant (S1). The detergent-insoluble pellet was extracted in lysis buffer (0.4% SDS, 500 mM NaCl, 5 mM EDTA, 1 mM dithiothreitol [DTT], 50 mM Tris-HCl, pH 7.4) (30 min, RT, gentle mixing) and a 5% sample taken (P1). The solubilized material was collected by centrifugation (16,000 × *g*, 10 min, RT) and a 5% sample taken of the supernatant (S2). Streptavidin-coated Dynabeads (approximately 100 μl per 50 ml of cell culture) were separately added to fractions S1 and S2 and incubated with gentle mixing (4 h, 4°C). The beads were separated from the unbound fraction by magnetic separation using a Dyna-Mag magnet. A 5% sample was taken of the two free unbound fractions (F1, F2). The Dynabeads were washed extensively with either PBS alone or the full wash procedure as described by Roux and coauthors (20). The Dynabeads were pelleted by centrifugation (6,000 × *g*, 2 min, RT). The beads (representing 100% of fractions B1 and B2) were resuspended in SDS-PAGE loading buffer and used directly for blotting. Equal fractions from each sample were separated by SDS-PAGE, transferred to nitrocellulose, and blotted with HRP-conjugated streptavidin. In bulk preparations intended for mass spectrometry analysis, the Dynabeads were added only to fraction S2. After the final centrifugation step, a 10% sample of the beads (fraction B2) was taken and separated electrophoretically by SDS-PAGE, and the protein concentration was estimated by silver staining. The remaining 90% was analyzed by mass spectrometry. Of the three bulk preparations, the first was conducted using the full wash procedure as detailed by Roux et al., the latter two using PBS washes only (20). Small-scale preparations were typically 50-ml cell cultures (approximately 5×10^8 cells); bulk preparations were 500-ml cell culture (approximately 5×10^9 cells).

Mass spectrometry (nano-liquid chromatography-tandem mass spectrometry [LC/MS-MS]) analysis. Beads were washed 5 times with 50 mM ammonium bicarbonate and then suspended in 100 μl ammonium bicarbonate. Disulfide bonds were reduced with 10% DTT (by weight of the estimated amount of protein) (30 min, 56°C) and subsequently alkylated with 50% iodoacetamide (by weight of the estimated amount of protein) (20 min, RT, in the dark). Then, 5% DTT (wt/wt of the estimated amount of protein) was added to consume excess iodoacetamide and proteins were digested with 5% trypsin (by weight of the estimated amount of protein) (recombinant, proteomics grade; Roche) (37°C, overnight). Digests were stopped by the addition of trifluoroacetic acid to approximately pH 2. Digests (5 to 10% of total) were analyzed on an UltiMate 3000 high-performance liquid chromatography (HPLC) system (Dionex; Thermo Fisher Scientific) coupled to an LTQ-Orbitrap Velos mass spectrometer (Thermo Fisher Scientific) via a nanoelectrospray ionization source (Proxeon; Thermo Fisher Scientific). Peptides were loaded on a trapping column (PepMap C_{18}, 5-μm particle size, 300 μm inner diameter, 5 mm length; Thermo Fisher Scientific) with 0.1% trifluoroacetic acid and separated on an analytical column (PepMap C_{18}, 3-μm particle size, 75 μm inner diameter, 150 mm length; Thermo Fisher Scientific) with a flow rate of 300 nl/min applying a 90-min linear gradient from 2.5% up to 40% acetonitrile. The voltage of the ion source was set to 1,500 V. The mass spectrometer was operated in the data-dependent mode: 1 full scan in the orbitrap (*m/z*, 400 to 1,800; resolution, 60,000) with lock mass (*m/z*, 445.120025) enabled was followed by a maximum of 20 MS-MS scans. Monoisotopic precursors were selected; singly charged signals were excluded from fragmentation. The collision energy was set at

35%, the Q value at 0.25, and the activation time at 10 ms. Fragmented ions were excluded from further selection for 30 s.

Mass spectrometry data interpretation. Raw spectra were interpreted by Mascot 2.2.04 (Matrix Science) using Mascot Daemon 2.2.2. Spectra were searched against the TriTryp database for T.brucei427 and T.brucei927 (18,355 entries, 23 April 2012; http://tritrypdb.org/) (24). The database was manually supplemented with the sequences of streptavidin and a set of frequent contaminants such as keratins and proteases. Search parameters were as follows: peptide tolerance, 2 ppm; fragment tolerance, 0.8 Da; trypsin specificity with two missed cleavages; carbamidomethyl cysteine as static; oxidation of methionine as variable modification. MASCOT results were loaded into Scaffold (version 3.00.02; Proteome Software). Peptide identifications were accepted when a minimum of two peptides were identified with a probability greater than 95% as assigned by the Protein Prophet algorithm; this resulted in a false discovery rate of 0%.

Candidate screening. Candidate genes were cloned into the pXS2 expression vector with a Ty1 epitope tag. The plasmids were introduced into cells by electroporation, and localizations were determined by immunofluorescence assay after an overnight incubation. Endogenous replacement of candidate genes to generate stably transfected cell lines was accomplished using previously published methods (19). The endogenous replacements encoded a triple Ty1 epitope tag at the 5′ end of the target allele and were screened by 10-μg/ml blasticidin selection. Integration of the targeting construct at the endogenous allele locus by double homologous recombination was confirmed by PCR amplification of genomic DNA, using primers that annealed within the epitope tag and outside the targeting fragment (see Fig. S2A in the supplemental material).

RESULTS

In order to generate trypanosome cells that inducibly expressed transgenes for BioID, the Myc-BirA* module was subcloned into the pLEW100 expression vector (23). This vector permits transgenes to be stably integrated into a ribosomal DNA (rDNA) locus and provides tetracycline-inducible control over expression of the encoded protein. The new expression vector was termed pLEW100_Myc_BirA*. The TbMORN1 open reading frame was then cloned into pLEW100_Myc_BirA* (Fig. 1A). Trypanosome cells from the 29-13 cell line were transfected with the construct, and stably transfected clones were obtained. The presence of the pLEW100_Myc_BirA*-TbMORN1 construct in the genomic DNA of the clones was confirmed by PCR (data not shown). Addition of tetracycline to the culture medium caused expression of an approximately 75-kDa polypeptide that was recognized by both anti-TbMORN1 and anti-Myc antibodies. No expression was seen in untransfected 29-13 control cells or uninduced cultures (Fig. 1B). It was concluded that Myc-BirA*-TbMORN1 was faithfully and inducibly expressed. Indirect immunofluorescence analysis confirmed the localization and morphology of Myc-BirA*-TbMORN1. Endogenous TbMORN1 has a fishhook-shaped expression pattern and localizes close to the point of flagellum entry into the cell (Fig. 1C, panel i). In intact cells there is also a small cytoplasmic fraction of TbMORN1. In detergent-extracted cells, TbMORN1 is present only at the bilobe (Fig. 1C, panel iii). Myc-BirA*-TbMORN1 was found to recapitulate the localization and morphology of endogenous TbMORN1 in both intact cells (Fig. 1C, panel ii) and detergent-extracted cells (Fig. 1C, panel iv). In the absence of tetracycline, no labeling was detected with the anti-Myc antibodies (data not shown). It was concluded that addition of the Myc-BirA* module did not interfere with correct localization. The induction of expression and correct localization of Myc-BirA*-TbMORN1, respectively, shown by immunoblotting and immunofluorescence assay, were demonstrated in two other independent clonal cell lines (data not shown). Culturing Myc-BirA*-TbMORN1-expressing cells at tetracycline concentrations between 0 and 10 ng/ml showed no effect on growth (data not shown). The Myc-BirA* module therefore appears to be nontoxic to trypanosome cells.

To determine whether the expressed Myc-BirA*-TbMORN1 caused biotinylation of candidate binding partners and near neighbors, the cells were cultured for 24 h in the presence of excess biotin and the presence or absence of tetracycline. Intact and detergent-extracted cells were labeled with anti-Myc antibodies and fluorescently conjugated streptavidin. In the presence of tetracycline, intact cells showed good labeling in both channels and strong overlap at the bilobe was clearly visible (Fig. 2A, arrows and insets). Both the anti-Myc and streptavidin labeling patterns closely resembled that seen for endogenous TbMORN1. Consistent with the data presented in Fig. 1C, in detergent-extracted cells the labeling was confined to the bilobe area. The anti-Myc and streptavidin signals strongly overlapped (Fig. 2C, arrows and insets). In the absence of tetracycline, intact cells showed no anti-Myc labeling and only a background signal from streptavidin (Fig. 2B). Detergent-extracted cells showed no significant signal with either label in the absence of tetracycline (Fig. 2D). Whole-cell lysates from both cell populations were analyzed by Western blotting. An HRP-conjugated streptavidin probe confirmed a significant increase in the number and quantity of biotinylated proteins in cells expressing Myc-BirA*-TbMORN1 (Fig. 2E, upper panel). Equal loading of lysates was confirmed by immunoblotting with antibodies specific for the flagellar pocket collar protein TbBILBO1 antibodies (Fig. 2E, lower panel). It was concluded that expression of Myc-BirA*-TbMORN1 in the presence of excess biotin caused biotinylation of candidate binding partners and near neighbors *in vivo*. These results were verified in two other independent clonal cell lines (data not shown).

It was decided to separately purify candidates from the detergent-soluble (cytoplasmic) and detergent-insoluble (cytoskeletal) fractions, as the primary goal of the project was to identify structural components of the bilobe. Such components were predicted to be tightly associated with the cytoskeleton, as is the case for TbMORN1 (15). A biochemical fractionation protocol was designed to accomplish this two-part purification (Fig. 3A). Comparison of equal fractions from cells expressing Myc-BirA*-TbMORN1 suggested that the protocol functioned according to design (Fig. 3B). The biotinylated proteins in the whole-cell input (E1) were efficiently partitioned into detergent-soluble (S1) and detergent-insoluble (P1) fractions. The detergent-insoluble fraction was effectively solubilized by SDS (S2). The unbound fraction of the cytoplasmic, detergent-soluble population (F1) contained a number of proteins indicating that in this preparation the streptavidin beads' binding capacity was probably saturated (compare F1 and S1). The unbound fraction of the cytoskeletal, detergent-insoluble population (F2) was largely depleted of biotinylated proteins, indicating good capture (compare F2 and S2). Despite the relatively good capture rates, both elutions (B1 and B2) displayed considerably less material relative to the inputs (S1 and S2). This was likely to be due to inefficient elution of the biotinylated proteins from the streptavidin beads. In both eluates, an approximately 75-kDa protein was clearly visible—immunoblots with anti-Myc antibodies showed that this was Myc-BirA*-TbMORN1 (data not shown). A large percentage of Myc-BirA*-TbMORN1

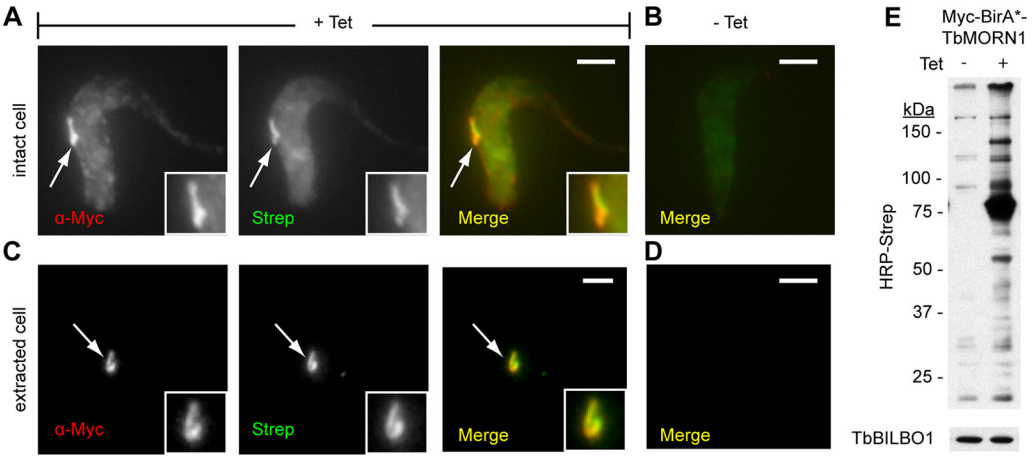

FIG 2 Biotinylation by Myc-BirA*-TbMORN1 *in vivo*. Myc-BirA*-TbMORN1 cells were incubated with excess biotin in the presence or absence of 10 ng/ml tetracycline (Tet). (A and B) Immunofluorescence assay of intact cells labeled with anti-Myc antibodies and fluorescently conjugated streptavidin. In the presence of tetracycline (A), the two labels strongly overlapped. The bilobe (arrows, area enlarged in insets) was clearly visible. In the absence of tetracycline (B), only endogenously biotinylated proteins were labeled as a background signal. (C and D) Immunofluorescence assay of detergent-extracted cells labeled as in panels A and B. In the presence of tetracycline (C), colocalization between the anti-Myc and streptavidin labels was seen at the bilobe (arrows, area enlarged in insets). In the absence of tetracycline (D), no labeling was observed in either channel. Images are maximum intensity z-projections; overlap was confirmed in single 0.1-μm sections. Identical exposure times and channel level settings were used in image acquisition and processing. Scale bars, 2 μm. (E) Immunoblot of whole-cell lysates using HRP-conjugated streptavidin. In the presence of tetracycline, many additional polypeptides are strongly biotinylated. Equal loading was confirmed by blotting the samples with anti-TbBILBO1 (lower panel).

partitions into the detergent-soluble fraction, due to the mild levels of overexpression. This is consistent with the amount of TbMORN1 present at the bilobe being a finite and saturable quantity (our unpublished observations). Comparison of purifications under experimental (+Tet) and control (−Tet) conditions revealed an extremely good signal-to-noise ratio (Fig. 3C). Eluates from control (−Tet) conditions showed virtually no biotinylated proteins whatsoever (Fig. 3C, left panel, fractions B1 and B2). Loading of larger fractions showed the presence of a number of candidates of defined molecular weights in the experimental condition elutions (Fig. 3C, right panel). Of particular interest, purifications from the detergent-insoluble, cytoskeletal fraction (B2) revealed three good candidates of approximately 79-, 90-, and 130-kDa molecular sizes in addition to Myc-BirA*-TbMORN1 (Fig. 3C, right panel). It was concluded that candidate TbMORN1 binding partners and near neighbors could be efficiently purified from Myc-BirA*-TbMORN1 cells and that uninduced (−Tet) cells represent an excellent control for nonspecific binding and background levels.

To identify candidate TbMORN1 binding partners and near neighbors from the detergent-insoluble, cytoskeletal fraction, bulk purifications were carried out in the presence of biotin and in the presence or absence of tetracycline. The eluates (B2) from both control and experimental samples were analyzed by mass spectrometry. To avoid the problem of inefficient elution of biotinylated proteins from the streptavidin-conjugated beads, the captured proteins were directly trypsinized on the beads. Three independent bulk purifications were carried out. Comparison of fractions from each of these purifications confirmed a high level of reproducibility (see Fig. S2B in the supplemental material). Promising candidate proteins were identified on the basis of having high scores (in terms of number of assigned spectra and number of unique peptides) in the experimental samples and low-to-zero scores in the control samples. The top-scoring protein in all three data sets was TbMORN1 itself. Significantly, TbLRRP1, which has been shown to colocalize with TbMORN1, scored as a strong hit (Table 1) (19). The flagellar pocket collar protein TbBILBO1, which only partially overlaps with TbMORN1, was not present. A total of 10 proteins were selected for screening, based on the following criteria: (i) high scores in terms of assigned spectra and unique peptides in all three experimental samples; (ii) low-to-zero scores in all three control samples; (iii) uncharacterized localization (Table 1). Many of these candidates had molecular weights corresponding to those of the proteins observed in the B2 elution fraction (Fig. 3C, right panel). A complete list of all high-scoring proteins across all three experiments is also provided (see Table S1 in the supplemental material). Included in the table are RNA interference (RNAi) phenotypes, as determined in the recent high-throughput screen of *T. brucei*, and information on whether the proteins are also represented in the *T. brucei* flagellum proteome (10, 25).

The localization of all 10 proteins in detergent-extracted cells was determined. This was accomplished either by transient expression of a Ty1 epitope-tagged version of the candidate or, in the case of larger or poorly transfecting candidates, by generation of endogenous replacement cell lines expressing the candidate with a triple Ty1 epitope tag. Expression of the tagged proteins was confirmed by immunoblots of whole-cell lysates with anti-Ty1 antibodies (Fig. 4A). For the largest two proteins (Tb927.10.1450 and Tb927.7.3330; 329 and 502 kDa, respectively), expression was confirmed by dot blot (Fig. 4B). All but one of the candidates exhibited a localization consistent with its designation as a TbMORN1 binding partner or near neighbor. Six proteins showed good overlap with TbMORN1 (Fig. 5). Two proteins (Tb927.10.3010 and Tb927.08.3010) strongly overlapped with TbMORN1 throughout its whole fishhook expression pattern (Fig. 5A and B). One protein was present throughout the whole fishhook shape but gave the strongest signal from the hooked pos-

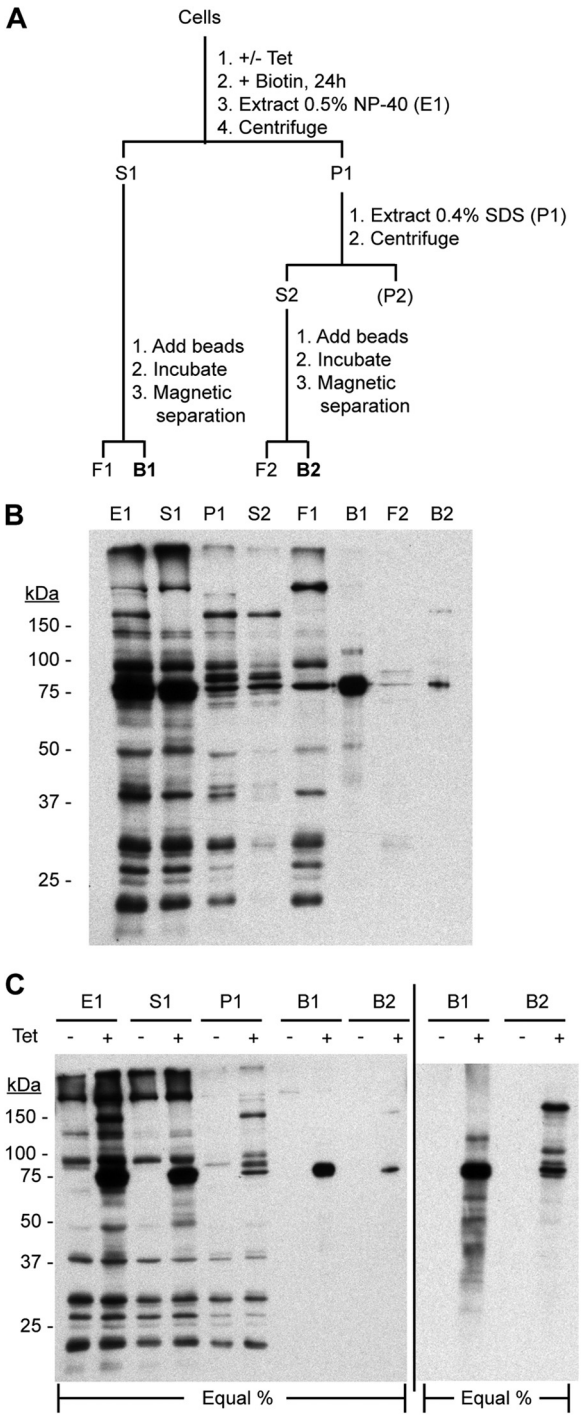

FIG 3 Purification of candidate TbMORN1 binding partners and near neighbors. (A) Schematic of purification protocol. Following incubation in excess biotin and the presence or absence of tetracycline (+/− Tet), the cells are incubated with 0.5% NP-40 (E1) and separated by centrifugation into detergent-soluble (S1) and detergent-insoluble (P1) fractions. The detergent-insoluble fraction is then further extracted with 0.4% SDS. Fractions S1 and S2 are incubated with streptavidin-conjugated paramagnetic beads, and the free unbound fractions (F1 and F2, respectively) are separated magnetically. Fractions B1 and B2 are, respectively, the bound cytoplasmic and cytoskeletal eluates and will contain candidate TbMORN1 binding partners and near neighbors. (B) Representative purification. Myc-BirA*-TbMORN1-expressing cells were processed as described for panel A. Samples were immunoblotted using HRP-conjugated streptavidin. Equal fractions were loaded in each lane. (C) Representative purification from Myc-BirA*-TbMORN1 cells incubated with excess biotin in either the presence or absence of tetracycline. Samples were immunoblotted using HRP-conjugated streptavidin; equal fractions in each lane. Comparison of +/− tetracycline conditions shows clear enrichment of biotinylated proteins in fractions E1, S1, and P1 and purification with minimal background in elutions B1 and B2 (left panel). Loading larger fractions of elutions B1 and B2 shows efficient capture of candidate TbMORN1 binding partners and near neighbors. Background signal from − Tet cells remains minimal (right panel).

terior part (Tb927.4.3120) (Fig. 5C). Two proteins (Tb927.7.7000 and Tb927.10.850) partially overlapped with TbMORN1 but showed an additional localization alongside it (Fig. 5D and E). Another protein (Tb927.10.8820) was localized solely to the stem anterior part of TbMORN1 (Fig. 5F). Three of the remaining proteins showed a localization that could be readily interpreted as indicating a binding partner or near neighbor of TbMORN1 (Fig. 6). One (Tb927.10.1450) was positioned alongside the stem anterior part of TbMORN1, much like TbCentrin4 (Fig. 6A). Two (Tb927.7.3330 and Tb927.4.5340) were localized to a punctate filamentous structure whose posterior end partially overlapped with the anterior stem of TbMORN1 (Fig. 6B and C). Only one candidate (Tb927.7.3740) appeared to be a false positive, which was defined as a protein whose localization disfavored its being a TbMORN1 binding partner or near neighbor. This candidate (Tb927.7.3740) was localized to the flagellum (Fig. 6D). The flagellum passes through the hook posterior part of TbMORN1 (producing an apparent partial overlap by immunofluorescence), but the flagellar proteins and bilobe proteins are insulated from one another by the flagellum membrane and flagellar pocket neck membrane. The localization of Tb927.7.3330 and Tb927.4.5340, with a partial overlap with the TbMORN1 bilobe, a punctate filamentous morphology, and a trajectory from the bilobe to the anterior end of the cell but not the tip of the flagellum, suggested FAZ localization. This was confirmed by colabeling with the FAZ-specific 1B41 monoclonal antibody (see Fig. S2C and D in the supplemental material).

Three of the candidates (Tb927.7.7000, Tb927.10.850, Tb927.10.1450) had localizations that suggested they might also partially or strongly overlap TbCentrin4. TbCentrin4 is primarily present on a bar that lies alongside the TbMORN1 fishhook, with a small amount extending toward the basal and probasal bodies where it is also localized. In addition, the protein (Tb927.10.8820) overlapping solely with the stem anterior part of TbMORN1 had an expression pattern strongly reminiscent of TbCentrin4. Colabeling experiments using anti-Ty1 and anti-TbCentrin4 antibodies confirmed a partial overlap with TbCentrin4 for Tb927.10.850 and Tb927.7.7000 (Fig. 7A and B). As expected, Tb927.10.1450 strongly overlapped with the TbCentrin4 bar, consistent with its localization alongside the stem anterior part of TbMORN1 (Fig. 7C). Tb927.10.8820 was found to mirror the TbCentrin4 bar (Fig. 7D).

DISCUSSION

BioID is a new and very powerful technique for identifying binding partners and near neighbors and was first used in mammalian tissue culture cells (20). The work described here demonstrates the successful adaptation of this technique to the parasitic protist *T. brucei*, using TbMORN1 to discover novel structural components of the trypanosome bilobe. The Myc-BirA* biotinylation module was found to be nontoxic and permissive for normal lo-

TABLE 1 Candidates shortlisted for evaluation of localization[a]

Accession no.	Molecular size (kDa)	No. of assigned spectra (no. of unique peptides)						% SC	Status[b]	Features[c]
		Expt 1		Expt 2		Expt 3				
		+Tet	−Tet	+Tet	−Tet	+Tet	−Tet			
Tb927.6.4670	41	235 (37)	0 (0)	136 (25)	0 (0)	324 (28)	2 (2)	71	TbMORN1	15× MORN
Tb927.10.3010	133	108 (63)	0 (0)	187 (59)	1 (1)	132 (54)	0 (0)	60	Unc	2× CC
Tb927.7.3330	502	63 (43)	0 (0)	21 (16)	2 (1)	34 (20)	2 (1)	7	Unc	13× CC
Tb11.01.0680	79	43 (26)	0 (0)	52 (25)	0 (0)	52 (24)	0 (0)	41	TbLRRP1	7× LRR, 1× CC
Tb927.7.3740	93	32 (27)	0 (0)	23 (19)	0 (0)	25 (18)	0 (0)	35	Unc	5× CC
Tb927.7.7000	176	31 (26)	0 (0)	41 (34)	0 (0)	29 (22)	0 (0)	20	Unc	
Tb927.10.1450	329	30 (23)	0 (0)	30 (19)	2 (1)	26 (22)	2 (2)	9	Unc	4× CC
Tb927.10.8820	85	24 (17)	0 (0)	60 (21)	1 (1)	26 (16)	1 (1)	27	Unc	
Tb927.10.850	168	20 (18)	0 (0)	27 (19)	0 (0)	26 (18)	0 (0)	15	Unc	5× WD40, 7× CC
Tb927.4.3120	101	18 (15)	0 (0)	29 (21)	0 (0)	23 (21)	0 (0)	27	Unc	
Tb927.4.5340	95	10 (10)	0 (0)	7 (7)	0 (0)	7 (7)	0 (0)	14	Unc	5× CC
Tb927.8.3010	82	3 (3)	0 (0)	9 (7)	1 (1)	11 (8)	1 (1)	10	Unc	3× CC

[a] Hits were ranked according to the number of assigned spectra in experiment 1; % sequence coverage (% SC) is shown, along with scores for assigned spectra and unique peptides under +/− Tet conditions.
[b] Unc, uncharacterized.
[c] MORN, membrane occupation and recognition nexus repeats; CC, predicted coiled-coil regions; LRR, predicted leucine-rich repeats; WD40, predicted WD40 repeat.

calization of tagged protein (Fig. 1). At approximately 35 kDa it is slightly larger than GFP, but it seems reasonable to assume that any protein whose localization is unaffected by GFP tagging could be utilized without handicap.

Incubation of Myc-BirA*-TbMORN1-expressing cells in excess biotin leads to the reproducible biotinylation of candidate proteins in the vicinity of the tagged bait (Fig. 2). Biotinylated proteins from both cytoplasmic and cytoskeletal fractions were efficiently purified and the latter subjected to analysis by mass spectrometry (Fig. 3). Comparison of the mass spectrometry data obtained from purifications in experimental/induced (+Tet) and control/uninduced (−Tet) conditions allowed subtraction of background binding and consequently the rapid selection of promising candidates. Screening a shortlist of candidates confirmed partial or strong overlap with TbMORN1 in the overwhelming majority of cases.

Most work on the trypanosome cytoskeleton has relied on a combination of light microscopy and electron microscopy coupled with phenotypic analysis following protein depletion by RNAi. Such work is, however, innately hampered by the difficulty of identifying candidate proteins to study and the inability to readily infer direct physical relationships between them. Both of these drawbacks relate to the fact that a large fraction of cytoskeletal and cytoskeleton-associated proteins are detergent insoluble and thus refractory to conventional affinity purification techniques. Tandem affinity purification (TAP) tagging techniques have become the benchmark method for identifying protein complexes but have an unavoidable requirement for detergent solubility of the complexes and sufficient strength and persistence of intracomplex interactions to withstand washing. The amount of material required may also be a limiting factor due to limited preservation of interacting partners. In the trypanosome cytoskeleton field, therefore, most protein identification efforts have focused on three approaches: (i) bioinformatic screens to identify orthologues of previously characterized proteins (26), (ii) generation of panels of monoclonal antibodies against entire elements of the cytoskeleton (27), and (iii) proteomic analysis of entire substructures of the cytoskeleton (10, 16, 28). The first method has the obvious drawback of being limited to identifying candidates with sequence/structural homology to other proteins, and this difficulty can also be compounded by the considerable evolutionary time separating trypanosomes (and other protists) from the better-studied members of the Eukaryota taxon. By definition, therefore, it cannot identify trypanosome-specific proteins. The second method is relatively unfocused owing to the large number of antigens present in even a substructure of the cytoskeleton, and identifying the target

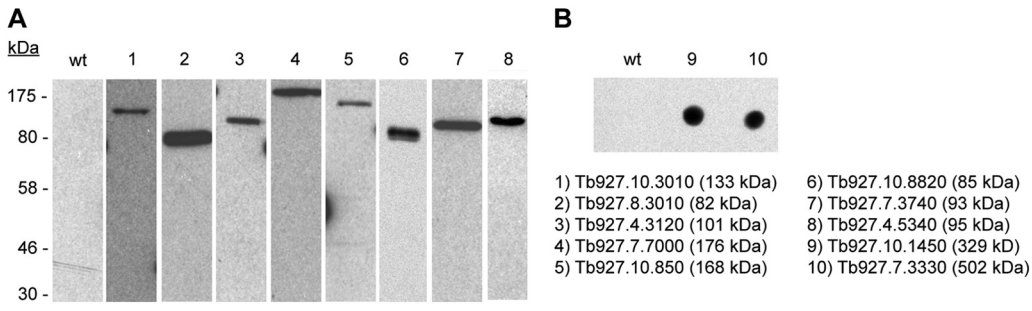

FIG 4 Confirmation of expression of tagged candidate proteins. Whole-cell lysates from cells expressing candidate TbMORN1 binding partners and near neighbors were analyzed by immunoblotting with anti-Ty1 antibodies. (A) Western blot of candidates. Expected molecular size is shown next to the figure. Addition of the Ty1 epitope tag causes a distinct decrease in electrophoretic mobility. (B) Dot blot of the two larger candidates.

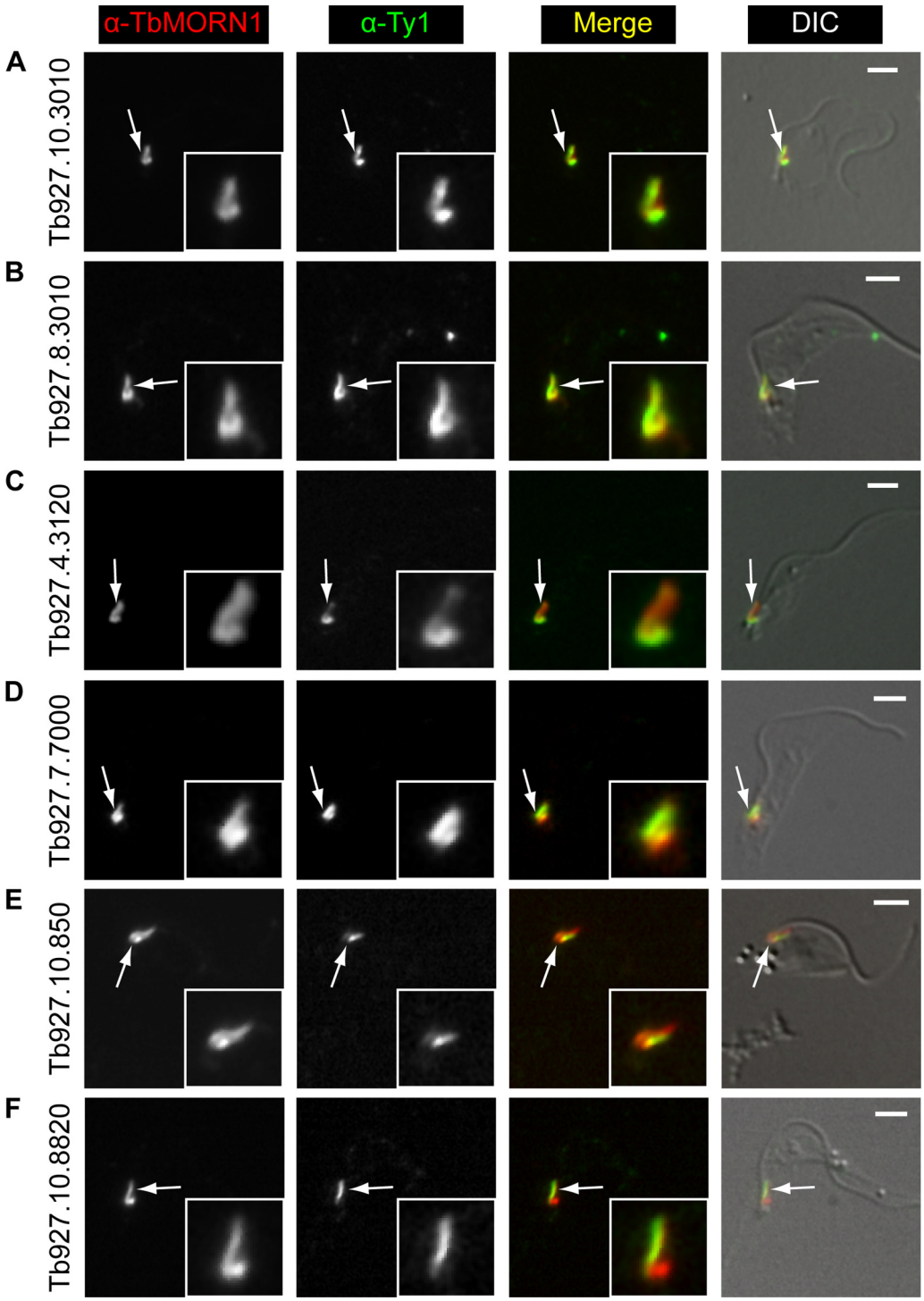

FIG 5 Localization of candidate proteins that overlap TbMORN1. Candidates were expressed with the Ty1 epitope tag in 427 cells either by transient transfection (first five rows) or endogenous replacement (last row). Detergent-extracted cells were labeled with anti-TbMORN1 and anti-Ty1 antibodies and analyzed by fluorescence microscopy. Single 0.1-μm z-slices are shown. Arrows indicate bilobe structure; area enlarged in insets. Fluorescence images were superimposed on differential interference contrast (DIC) images. The candidates localized either to the whole TbMORN1 bilobe (Tb927.10.3010, Tb927.8.3010) (A and B), primarily to the hook posterior part of TbMORN1 (Tb927.4.3120) (C), to both the bilobe and the adjacent TbCentrin4 arm (Tb927.7.7000, Tb927.10.850) (D and E), and to the posterior stem of TbMORN1 (Tb927.10.8820) (F). Scale bars, 2 μm.

antigen of a given monoclonal antibody remains far from trivial (29). The third method is comprehensive in that it can faithfully provide an entire inventory of constituent proteins but provides no information on the relationships between these proteins and no easy way to evaluate possible contaminants. Given that there are hundreds of different proteins in the flagellum alone, establishing such relationships can become a formidable task. Another method of screening for direct interactions of detergent-insoluble

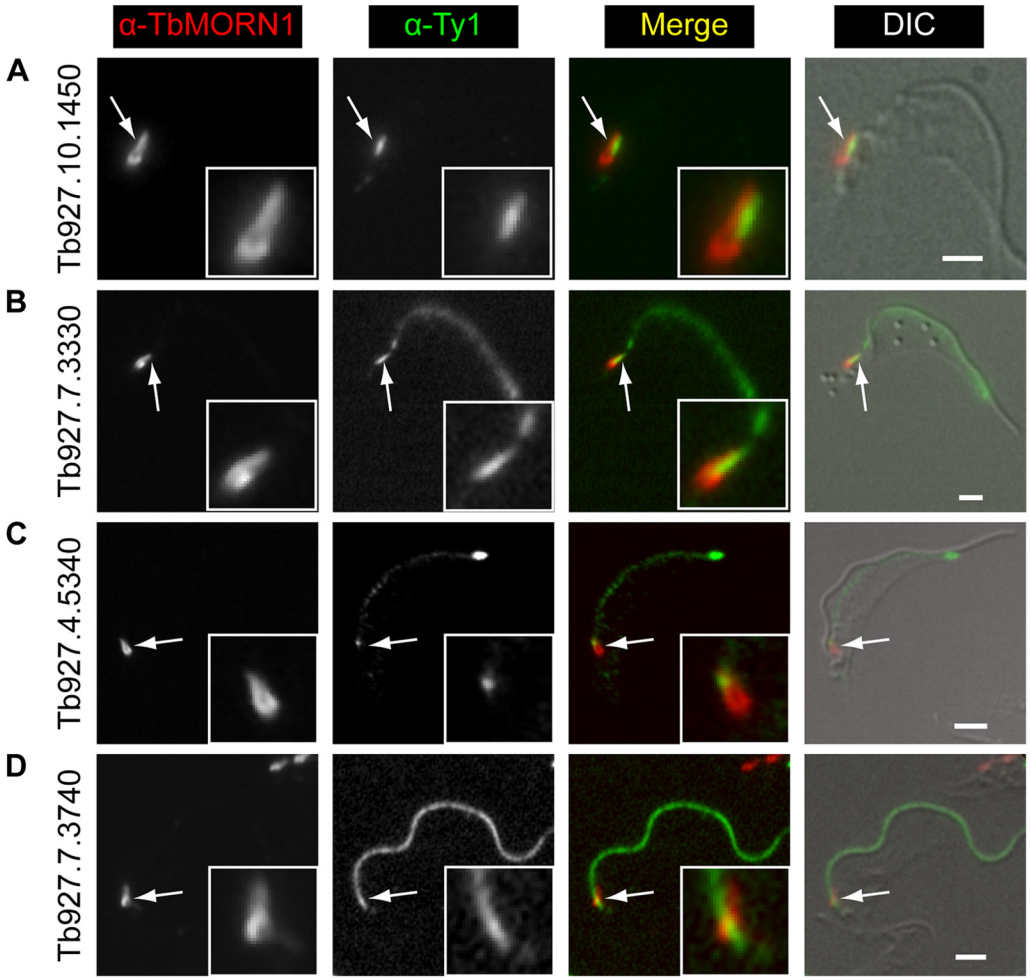

FIG 6 Localization of candidate proteins to the bilobe, FAZ, and flagellum. Candidates were expressed with the Ty1 epitope tag in 427 cells either by endogenous replacement (first two rows) or transient transfection (last two rows). Detergent-extracted cells were labeled with anti-TbMORN1 and anti-Ty1 antibodies and analyzed by fluorescence microscopy. Tb927.10.1450 was localized adjacent to the anterior stem part of TbMORN1 (A). Tb927.7.3330 and Tb927.4.5340 were present on the FAZ and showed partial overlap with TbMORN1 (B and C). Tb927.7.3740 was present on the flagellum (D). Single 0.1-μm z-slices are shown. Arrows indicate bilobe structure; area enlarged in insets. Fluorescence images were superimposed on DIC images. Scale bars, 2 μm.

proteins, the yeast two-hybrid technique, requires nonnative conditions and frequently generates false positives.

These results constitute an emphatic validation of BioID as a method for forward biochemical screens of binding partners and near neighbors. TbMORN1 has provided an exemplary test case for the technique. It is tightly associated with the trypanosome cytoskeleton, and it localizes to the bilobe—a discrete (approximately 2-μm long) structure of unclear function and almost completely unknown composition. Attempts to identify other bilobe proteins on the basis of homology have proved fruitless to date (our unpublished data). Here, using BioID has permitted the identification of at least seven new bilobe-resident proteins. In addition, two novel FAZ proteins were identified. All of the proteins here identified were previously experimentally uncharacterized, and none are homologous to TbMORN1 and TbLRRP1. All are specific to either the trypanosomes or the TriTryps, and they exhibit no common structural features other than a preponderance of coiled-coil and repeat regions. As such, it is highly unlikely that they would ever have been detected using *in silico* methods. All are detergent insoluble and consequently are highly unlikely to have ever been detected using conventional affinity purification techniques.

The presence of at least two FAZ proteins in this data set reinforces the idea that there is a close physical association of the bilobe and the FAZ. An overlap has previously been noted between the stem anterior part of TbMORN1 and the posterior end of the FAZ at both immunofluorescence and electron microscopy levels (15, 19). Similarly, the varied and overlapping distribution of the new bilobe proteins lends weight to the hypothesis that the structure is composed of subdomains rather than being a single homogeneous entity. It is curious that TbCentrin4 was not present in the list of candidates, especially given that Tb927.10.1450 overlapped with it. This could be due to a combination of the high number (i.e., 18) and small size of its predicted tryptic peptides within its 149-amino-acid primary sequence, disfavoring it for mass spectrometry identification. However, it also could not be detected in Western blots of the eluates, so it seems likely that a more complex explanation is involved (data not shown). On a related note, the absence of the flagellar pocket collar protein TbBILBO1 indirectly supports the notion that the flagellar pocket

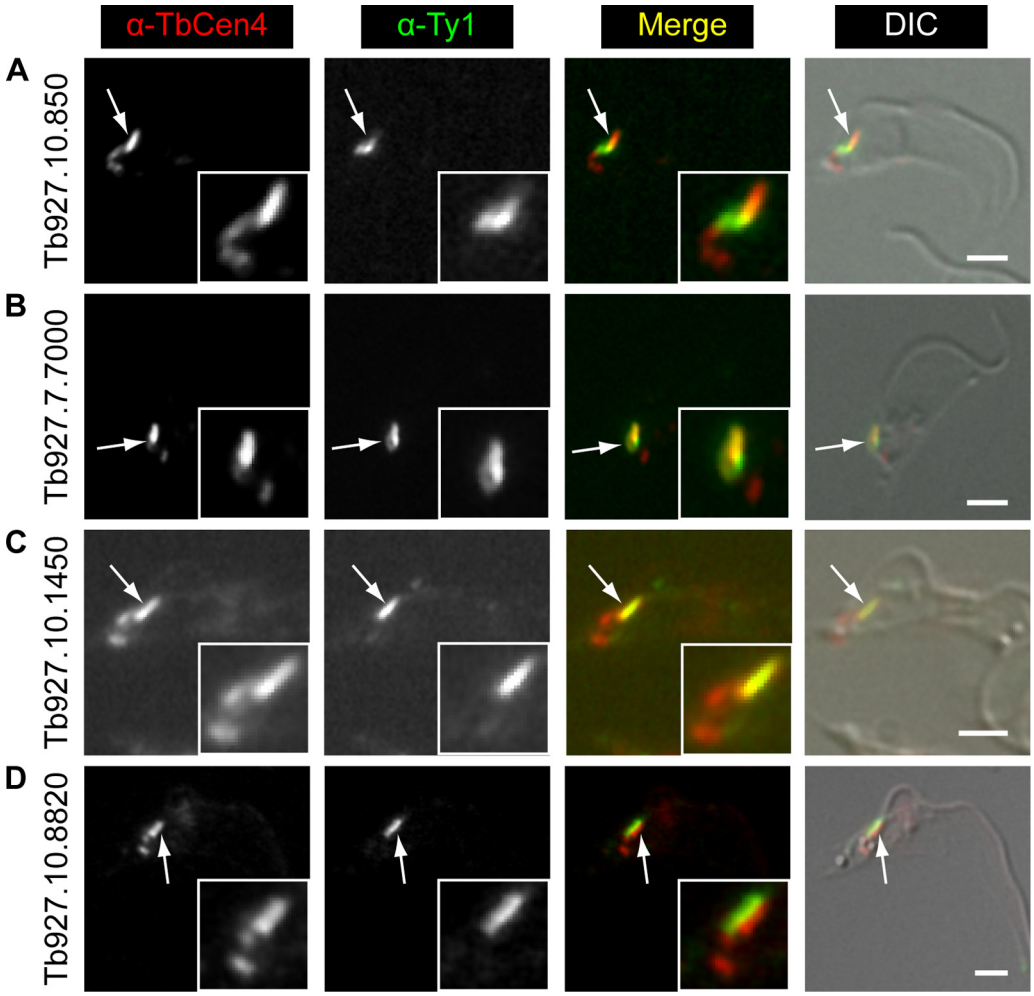

FIG 7 Localization of candidate TbMORN1 binding partners relative to TbCentrin4. Candidates were expressed with the Ty1 epitope tag in 427 cells either by transient transfection (first two rows) or endogenous replacement (last two rows). Detergent-extracted cells were labeled with anti-TbCentrin4 and anti-Ty1 antibodies and analyzed by fluorescence microscopy. Single 0.1-μm z-slices are shown. Arrows indicate bilobe structure; area enlarged in insets. Fluorescence images were superimposed on DIC images. As expected, Tb927.10.850 and Tb927.7.7000 showed a partial overlap with TbCentrin4 (A and B). Tb927.10.1450 (C) and Tb927.10.8820 (D) showed good and no overlap, respectively. Scale bars, 2 μm.

collar and the bilobe are distinct structures (19). The various localizations at the bilobe of the screened candidates have been summarized schematically (Fig. 8). It seems likely that the bilobe is composed of at least four subdomains—the whole fishhook-shaped structure (Fig. 8, panel 1), its anterior stem (Fig. 8, panel 2), its posterior hook (Fig. 8, panel 4), and the TbCentrin4 bar (Fig. 8, panel 3). In addition, a number of proteins are present at least partially on both the TbMORN1 fishhook and the TbCentrin4 bar, covering the entire bilobe (Fig. 8, panel 5). The anterior parts overlap the posterior end of the FAZ (Fig. 8, panel 6). These new findings extend our previous morphological work (19). Exploring these subdomains and teasing out the functional roles of the individual proteins within them represents an exciting future program of work. The priority in this study was to identify core structural components of the bilobe rather than more labile ones, but it will be interesting also to determine the composition of the detergent-soluble biotinylated fractions obtained in the experiments.

A final curiosity is why Tb927.7.3740 scored so highly when it is not localized to the bilobe. The protein registered as a good hit in all three independent purifications, better even than a number of the confirmed hits. A possible explanation is that the protein is in fact a binding partner of TbMORN1 but only a transient one. During early stages of the cell cycle, TbMORN1 and TbLRRP1 have been localized to tendrillar protein fibers that connect the bilobe and the basal body and probasal body (19). It is possible that there is a transient association between TbMORN1 and Tb927.7.3740 in this interval. Again, further work is required to clarify the question.

In conclusion, the results here validate the use of the BioID methodology in *T. brucei*. Although promiscuous biotinylation by BirA* was first demonstrated in *Escherichia coli*, the data here constitute—to our knowledge—the first demonstration of proximity-dependent BioID in nonhuman eukaryotic cells (30). Unlike the proof-of-principle experiments conducted on lamin-A in the comparatively well-characterized mammalian nuclear envelope, they are also the first application of BioID to an extranuclear structure about which very little is known. The success of BioID in

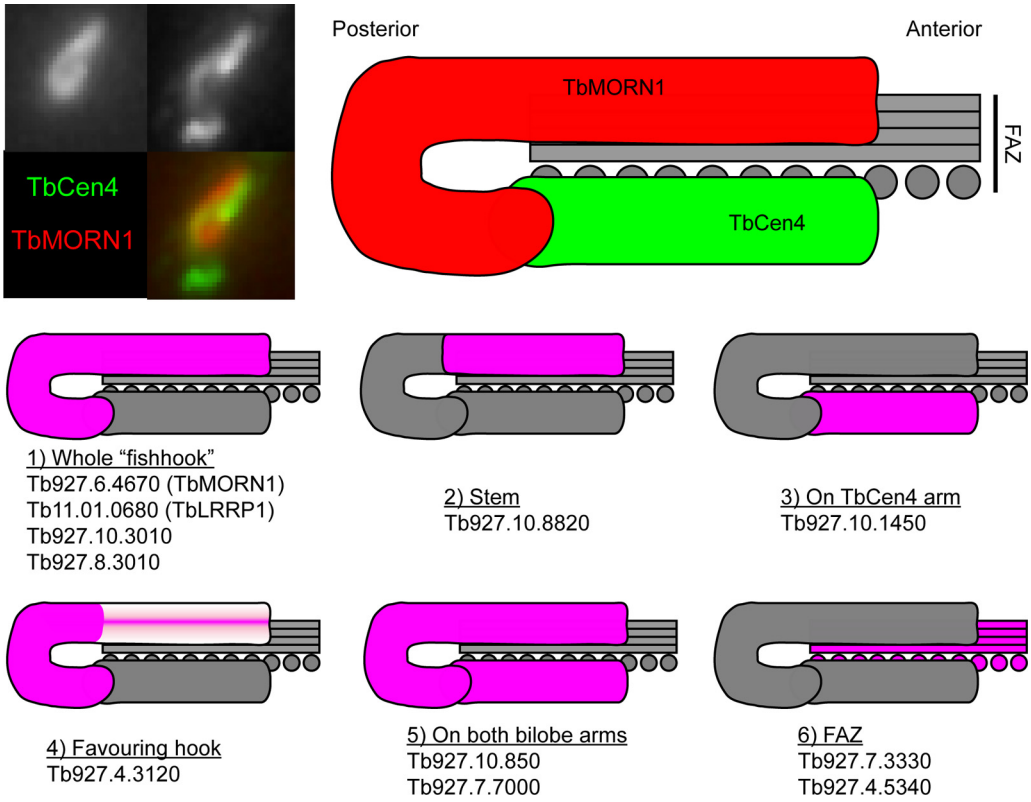

FIG 8 Schematic summarizing localizations of candidate TbMORN1 binding partners and near neighbors. The image at top left shows a close-up of the bilobe area from a detergent-extracted cell labeled with anti-TbMORN1 and anti-TbCentrin4. Dimensions of the schematic are taken from immunofluorescence images. TbCentrin4 localizations to the basal body and probasal body and the extra density extending from the bar toward the basal body are excluded for clarity.

identifying new components of that structure is very encouraging. Given that the only requirement for the technique is the capability for transgene expression, it is likely to be particularly suited to the study of protists (parasitic and otherwise) and other simpler eukaryotes where the level of genome annotation is low and the amount of evolutionary time separating them from standard model organisms such as mice and fruit flies inhibits easy bioinformatic identification of orthologues. Starting with only a single probe protein, BioID could in principle be used to bootstrap through the members of a protein complex or interaction network. The cytoskeletal field, frequently burdened with large and insoluble proteins, should benefit in particular.

ACKNOWLEDGMENTS

Funding was from the FWF Austrian Science Fund (FWF grant P22276-B12).

We thank Gustav Ammerer for assistance with mass spectrometry and Rainer Gith and other members of the mass spectrometry facility. We thank also Brian Burke (Institute of Medical Biology, Singapore) and the other members of the Warren lab for critical discussion of the manuscript.

REFERENCES

1. **Gull K.** 1999. The cytoskeleton of trypanosomatid parasites. Annu. Rev. Microbiol. **53**:629–655. doi:10.1146/annurev.micro.53.1.629.
2. **Robinson DR, Sherwin T, Ploubidou A, Byard EH, Gull K.** 1995. Microtubule polarity and dynamics in the control of organelle positioning, segregation, and cytokinesis in the trypanosome cell cycle. J. Cell Biol. **128**:1163–1172.
3. **Lacomble S, Vaughan S, Gadelha C, Morphew MK, Shaw MK, McIntosh JR, Gull K.** 2009. Three-dimensional cellular architecture of the flagellar pocket and associated cytoskeleton in trypanosomes revealed by electron microscope tomography. J. Cell Sci. **122**:1081–1090. doi:10.1242/jcs.045740.
4. **Engstler M, Thilo L, Weise F, Grunfelder CG, Schwarz H, Boshart M, Overath P.** 2004. Kinetics of endocytosis and recycling of the GPI-anchored variant surface glycoprotein in Trypanosoma brucei. J. Cell Sci. **117**:1105–1115. doi:10.1242/jcs.00938.
5. **Lacomble S, Vaughan S, Gadelha C, Morphew MK, Shaw MK, McIntosh JR, Gull K.** 2010. Basal body movements orchestrate membrane organelle division and cell morphogenesis in Trypanosoma brucei. J. Cell Sci. **123**:2884–2891. doi:10.1242/jcs.074161.
6. **Gull K.** 2003. Host-parasite interactions and trypanosome morphogenesis: a flagellar pocketful of goodies. Curr. Opin. Microbiol. **6**:365–370.
7. **Henley GL, Lee CM, Takeuchi A.** 1978. Electron microscopy observations on Trypanosoma brucei: freeze-cleaving and thin-sectioning study of the apical part of the flagellar pocket. Z Parasitenkd. **55**:181–187.
8. **Sherwin T, Gull K.** 1989. The cell division cycle of Trypanosoma brucei brucei: timing of event markers and cytoskeletal modulations. Philos. Trans. R. Soc. Lond. B Biol. Sci. **323**:573–588.
9. **Vickerman K.** 1969. On the surface coat and flagellar adhesion in trypanosomes. J. Cell Sci. **5**:163–193.
10. **Broadhead R, Dawe HR, Farr H, Griffiths S, Hart SR, Portman N, Shaw MK, Ginger ML, Gaskell SJ, McKean PG, Gull K.** 2006. Flagellar motility is required for the viability of the bloodstream trypanosome. Nature **440**:224–227. doi:10.1038/nature04541.
11. **Ralston KS, Kisalu NK, Hill KL.** 2011. Structure-function analysis of dynein light chain 1 identifies viable motility mutants in bloodstream-form Trypanosoma brucei. Eukaryot. Cell **10**:884–894. doi:10.1128/EC.00298-10.
12. **Zhou Q, Liu B, Sun Y, He CY.** 2011. A coiled-coil- and C2-domain-containing protein is required for FAZ assembly and cell morphology in Trypanosoma brucei. J. Cell Sci. **124**:3848–3858. doi:10.1242/jcs.087676.
13. **May SF, Peacock L, Almeida Costa CI, Gibson WC, Tetley L, Robinson DR, Hammarton TC.** 2012. The Trypanosoma brucei AIR9-like protein is

cytoskeleton-associated and is required for nucleus positioning and accurate cleavage furrow placement. Mol. Microbiol. **84**:77–92. doi:10.1111/j.1365-2958.2012.08008.x.

14. **He CY, Pypaert M, Warren G.** 2005. Golgi duplication in Trypanosoma brucei requires Centrin2. Science **310**:1196–1198. doi:10.1126/science.1119969.
15. **Morriswood B, He CY, Sealey-Cardona M, Yelinek J, Pypaert M, Warren G.** 2009. The bilobe structure of Trypanosoma brucei contains a MORN-repeat protein. Mol. Biochem. Parasitol. **167**:95–103. doi:10.1016/j.molbiopara.2009.05.001.
16. **Zhou Q, Gheiratmand L, Chen Y, Lim TK, Zhang J, Li S, Xia N, Liu B, Lin Q, He CY.** 2010. A comparative proteomic analysis reveals a new bi-lobe protein required for bi-lobe duplication and cell division in Trypanosoma brucei. PLoS One **5**:e9660. doi:10.1371/journal.pone.0009660.
17. **Shi J, Franklin JB, Yelinek JT, Ebersberger I, Warren G, He CY.** 2008. Centrin4 coordinates cell and nuclear division in T. brucei. J. Cell Sci. **121**:3062–3070. doi:10.1242/jcs.030643.
18. **Wang M, Gheiratmand L, He CY.** 2012. An interplay between Centrin2 and Centrin4 on the bi-lobed structure in Trypanosoma brucei. Mol. Microbiol. **83**:1153–1161. doi:10.1111/j.1365-2958.2012.07998.x.
19. **Esson HJ, Morriswood B, Yavuz S, Vidilaseris K, Dong G, Warren G.** 2012. Morphology of the trypanosome bilobe, a novel cytoskeletal structure. Eukaryot. Cell **11**:761–772. doi:10.1128/EC.05287-11.
20. **Roux KJ, Kim DI, Raida M, Burke B.** 2012. A promiscuous biotin ligase fusion protein identifies proximal and interacting proteins in mammalian cells. J. Cell Biol. **196**:801–810. doi:10.1083/jcb.201112098.
21. **Lane MD, Young DL, Lynen F.** 1964. The enzymatic synthesis of holotranscarboxylase from apotranscarboxylase and (+)-biotin. I. Purification of the apoenzyme and synthetase; characteristics of the reaction. J. Biol. Chem. **239**:2858–2864.
22. **Kwon K, Beckett D.** 2000. Function of a conserved sequence motif in biotin holoenzyme synthetases. Protein Sci. **9**:1530–1539. doi:10.1110/ps.9.8.1530.
23. **Wirtz E, Leal S, Ochatt C, Cross GA.** 1999. A tightly regulated inducible expression system for conditional gene knock-outs and dominant-negative genetics in Trypanosoma brucei. Mol. Biochem. Parasitol. **99**:89–101.
24. **Aslett M, Aurrecoechea C, Berriman M, Brestelli J, Brunk BP, Carrington M, Depledge DP, Fischer S, Gajria B, Gao X, Gardner MJ, Gingle A, Grant G, Harb OS, Heiges M, Hertz-Fowler C, Houston R, Innamorato F, Iodice J, Kissinger JC, Kraemer E, Li W, Logan FJ, Miller JA, Mitra S, Myler PJ, Nayak V, Pennington C, Phan I, Pinney DF, Ramasamy G, Rogers MB, Roos DS, Ross C, Sivam D, Smith DF, Srinivasamoorthy G, Stoeckert CJ, Subramanian S, Thibodeau R, Tivey A, Treatman C, Velarde G, Wang H.** 2010. TriTrypDB: a functional genomic resource for the Trypanosomatidae. Nucleic Acids Res. **38**:D457–D462. doi:10.1093/nar/gkp851.
25. **Alsford S, Turner DJ, Obado SO, Sanchez-Flores A, Glover L, Berriman M, Hertz-Fowler C, Horn D.** 2011. High-throughput phenotyping using parallel sequencing of RNA interference targets in the African trypanosome. Genome Res. **21**:915–924. doi:10.1101/gr.115089.110.
26. **Absalon S, Blisnick T, Kohl L, Toutirais G, Dore G, Julkowska D, Tavenet A, Bastin P.** 2008. Intraflagellar transport and functional analysis of genes required for flagellum formation in trypanosomes. Mol. Biol. Cell **19**:929–944. doi:10.1091/mbc.E07-08-0749.
27. **Bonhivers M, Nowacki S, Landrein N, Robinson DR.** 2008. Biogenesis of the trypanosome endo-exocytotic organelle is cytoskeleton mediated. PLoS Biol. **6**:e105. doi:10.1371/journal.pbio.0060105.
28. **Portman N, Lacomble S, Thomas B, McKean PG, Gull K.** 2009. Combining RNA interference mutants and comparative proteomics to identify protein components and dependences in a eukaryotic flagellum. J. Biol. Chem. **284**:5610–5619. doi:10.1074/jbc.M808859200.
29. **Vaughan S, Kohl L, Ngai I, Wheeler RJ, Gull K.** 2008. A repetitive protein essential for the flagellum attachment zone filament structure and function in Trypanosoma brucei. Protist **159**:127–136. doi:10.1016/j.protis.2007.08.005.
30. **Cronan JE.** 2005. Targeted and proximity-dependent promiscuous protein biotinylation by a mutant Escherichia coli biotin protein ligase. J. Nutr. Biochem. **16**:416–418. doi:10.1016/j.jnutbio.2005.03.017.